Numerical Simulation of Tidal Flooding over Mangrove Swamps

Shahbudin Saad[1], Mohd. Lokman Husain[2], Toshiyuki Asano[3],

[1]Borneo Marine Research Institute, Universiti Malaysia Sabah
Locked Bag No. 2073, 88999 Kota Kinabalu, Sabah, MALAYSIA

[2]Institute of Oceanography, Malaysian University College of Science and Technology (KUSTEM), Mengabang Telipot, 21030 Kuala Terengganu, MALAYSIA

[3]Department of Ocean Civil Engineering, Kagoshima University
Korimoto, Kagoshima, 890-0065, JAPAN

ABSTRACT. *Tidal flooding over mangrove swamps is subject to the drag resistance produced by mangrove roots, fallen branches, seedlings and mangrove bed conditions. A numerical study has been carried out to simulate the tidal flow over mangrove swamps in an estuarine mangrove, Kemaman Terengganu. This study aims to understand the characteristics of tidal level variations and velocity fields under the influence of the complex morphology and densely mangrove roots system. The two-dimensional finite difference model is used in this study. Results indicated that there is phase lag among the creeks because the distance from the estuary varies among each creek. At a cross-section J110, an overflow occurs over adjacent two creeks faster than the left one at a maximum water level around T = 20hr. Meanwhile, in the right creek the highest water level occurs at T = 18hr. The calculation shows that the flooding (at 18hr 40min) enters deeper inside the mangrove swamps if the flood plain is assumed to have no mangrove roots resistance except the bed friction.*

Keywords: Flooding flows, estuarine mangrove, mangrove swamps, drag resistance

INTRODUCTION

Mangroves are very unique ecosystem among the coastal habitats that inhabit mostly the sheltered coastlines within the inter-tidal zone of tropical and subtropical region. It plays a multidisciplinary role in various aspects. For coastal engineers, mangrove are reckoned as a buffer zone due to their presumed important functions in reducing wave energy, providing mechanisms for trapping sediments and reducing the risk of shoreline erosion (Saad *et. al*., 1999; Furukawa and Wolanski, 1996; Stumpf, 1983).

Hydrodynamic process of tidal flows over mangrove flood plains plays important roles in the structure and function of a mangrove ecosystem. This process become very unique and complicated due to the morphology of mangroves that usually comprised of narrow and branched creeks and complex branched roots system (Asano, *et al*., 2000). The importance of hydrodynamics process of tidal flows that directly governs other activities such as biological, chemical and physical has been widely recognized, however, the present understanding is not satisfactory. Realizing the lack of data and information concerning the hydrodynamics and having considered the potential of mangroves in various aspects of the environment, this study is important to be done. The main objective of this study is to develop a numerical model to reproduce a tidal flow in the Kemaman mangrove estuary. Two series of calculation have been conducted in order to evaluate the retarding effects. The calculations are made by including and excluding the mangrove roughness effects.

DESCRIPTION OF THE STUDY AREA

The study area located in the district of Kemaman (Lat. 4° 14′ N, Long. 103° 25′ E), which is lies to the east coast of Peninsular Malaysia, approximately 170 km south of Kuala Terengganu. It has a wide

distribution of mangroves about 938 ha along the Kemaman and Chukai river, especially along the southern bank of Kemaman estuary (Figure 1). The tide is semidiurnal with a mean range of 1.8 m and floods the area twice daily. However, total inundation of the mangrove area occurs only during spring tides, when water rises to approximately 2.6 m. The average freshwater discharge of Kemaman River is higher during Northeast monsoon (500 m^3s^{-1}) compared to Southwest monsoon (80 m^3s^{-1}). The mean annual rainfall is 3064mm in which high rainfall occurred during Northeast monsoon. According to the Malaysian Meteorological Service Department, strong winds with a long frequency periods occurred from November to January and from May to July. Fifty percent of the winds are from Northeasterly and Southwesterly direction. The Northeasterly wind coincides with the incoming wind normal to the coast of Kemaman bay. The maximum velocities for the Northeasterly winds are relatively higher than Southwesterly winds with a mean velocity 5.5 – 7.8 ms^{-1} and 3.4 – 5.4 ms^{-1} respectively.

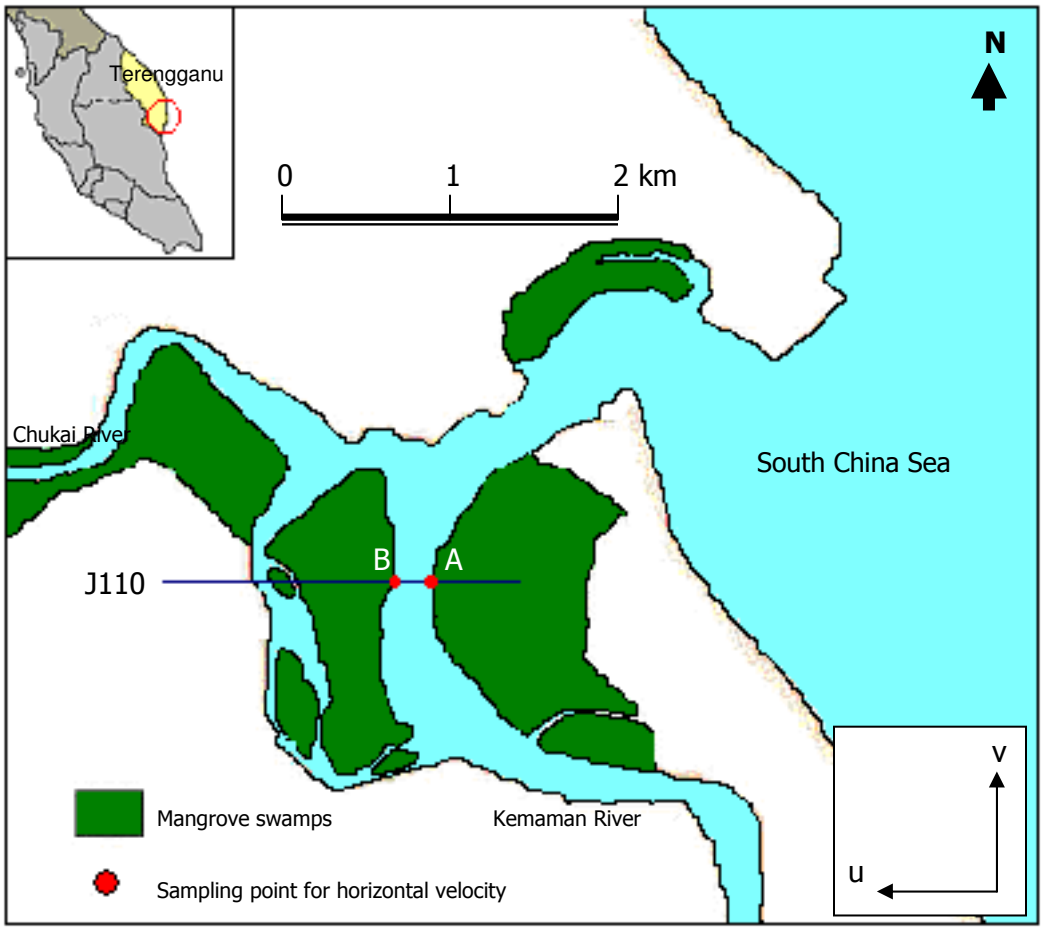

Figure 1. Sampling Stations

MATHEMATICAL MODEL

Two-dimensional finite difference model which is based on a Leapfrog scheme was used in this study. The basic equations are non-linear shallow water equations as follows:

$$\frac{\partial \eta}{\partial t} + \frac{\partial M}{\partial x} + \frac{\partial N}{\partial y} = 0 \quad (1)$$

$$\frac{\partial M}{\partial t} + \frac{\partial}{\partial x}\frac{M^2}{D} + \frac{\partial}{\partial y}\frac{MN}{D} + gD\frac{\partial \eta}{\partial x} - f\frac{MQ}{D^2} - A_h\left(\frac{\partial^2 M}{\partial x^2} + \frac{\partial^2 M}{\partial y^2}\right) = 0 \quad (2)$$

$$\frac{\partial N}{\partial t} + \frac{\partial}{\partial x}\frac{MN}{D} + \frac{\partial}{\partial y}\frac{N^2}{D} + gD\frac{\partial \eta}{\partial y} - f\frac{NQ}{D^2} - A_h\left(\frac{\partial^2 N}{\partial x^2} + \frac{\partial^2 N}{\partial y^2}\right) = 0 \quad (3)$$

where, $D = h + \eta$ is the total depth (h: still water depth, η: water surface elevation), (M, N) = (Du, Dv) and $Q = \sqrt{M^2 + N^2}$ are the mass fluxes. A_h is the horizontal mixing coefficient and it is used as 1.0 m^2/s. The friction factor f comprised of the bottom friction f_b and the drag resistance due to the mangrove roots f_{roots} (Asano, 1999) as follow:

$$f = f_b + f_{roots}, \quad f_{roots} = \frac{1}{2} C_D \int_0^D d_0(z) N(z) dz \quad (4)$$

where, C_D is the drag coefficient, d_0 is the projected diameter of a mangrove root, N is the number of roots per unit bottom area and $A(z)$ is sum of the projected area of mangrove roots against the flow. Substituting equation (4) into the friction terms of equation (2) and (3) and integrating over the bottom area, we find

$$\rho \iint f \frac{MQ}{D^2} dxdy = \tau_{b,x} + \frac{\rho}{2} C_D A(z) u \sqrt{u^2 + v^2} \quad (5)$$

$$\rho \iint f \frac{NQ}{D^2} dxdy = \tau_{b,x} + \frac{\rho}{2} C_D A(z) v \sqrt{u^2 + v^2} \quad (6)$$

The calculation domain for the study area has been chosen as 4.3 km x 4.3 km square region. This region is divided into 280 x 280 computational grids, which result in 15.35 m for every grid size.

RESULT AND DISCUSSION

Figure 2 clearly shows the phase lag among the creeks (at cross-section J110) because the total distance from the estuary mouth varies at each case. The water level at the right creek rises up faster than that of the left at T=18hr. An overflow from the right side to the left side can be observed at that time. The water flooding continues until the water level start to recede. It is noted from the curves at T= 20hr that the water level in the right creek recedes faster than the left one.

Figure 3 elucidates the horizontal velocity distribution at point A (I118, J110) which is situated almost at the middle of estuary approximately 1.5km from river mouth. The small velocity at this point is due to the friction at the shallow water in this area that caused a diminution in the tidal range and flow velocity. Horizontal u-velocity is less than v-velocity. As illustrates in Figure 3, the maximum u-velocity during flood tide and ebb tide is just about 0.1m/s and 0.22m/s respectively. Meanwhile, the maximum v-velocity during flood tide and ebb tide is about 0.25m/s and 0.15m/s, respectively.

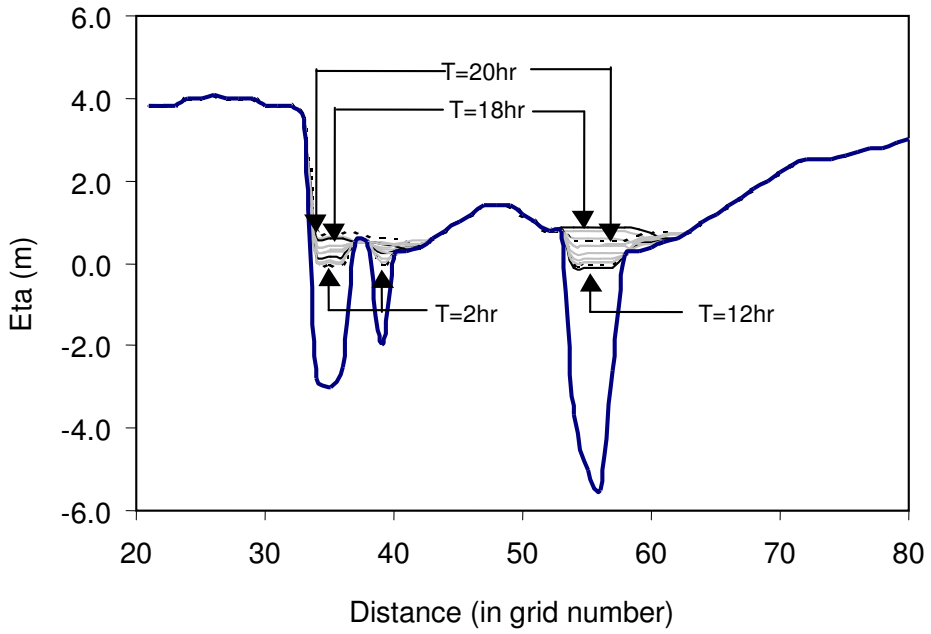

Figure 2: Surface Water Level Variation at Cross-section J110

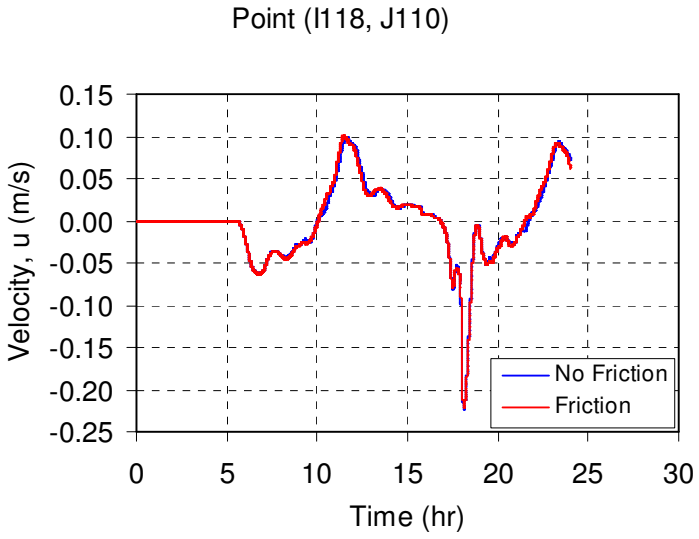

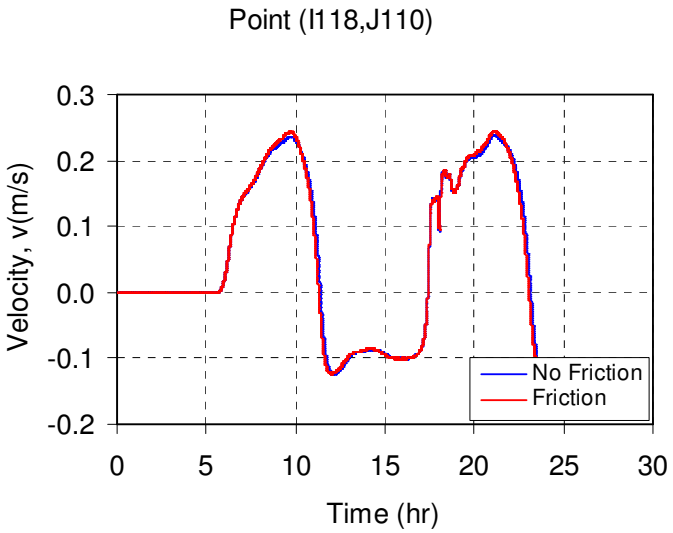

Figure 3: Horizontal u-Velocity and v-velocity Profiles at Point A (I118, J110) for Flooding and Non-flooding Cases

A flooding flow over a mangrove swamp is subject to the drag resistance by mangrove prop roots, pneumatophors and their fallen branches, seedlings and leaves etc. Generated low velocity region over the swamp will retard the adjacent velocity in the creak region by the lateral mixing effect. Figure 4 illustrates velocity variation for *u* and *v* at the central point B (I112) of the transect J110. Figures indicate that the peak values take greater values, even though the differences are small, for the case including mangrove roughness effects. This is the contrary result to that was expected from the resistance function by the mangrove roots system.

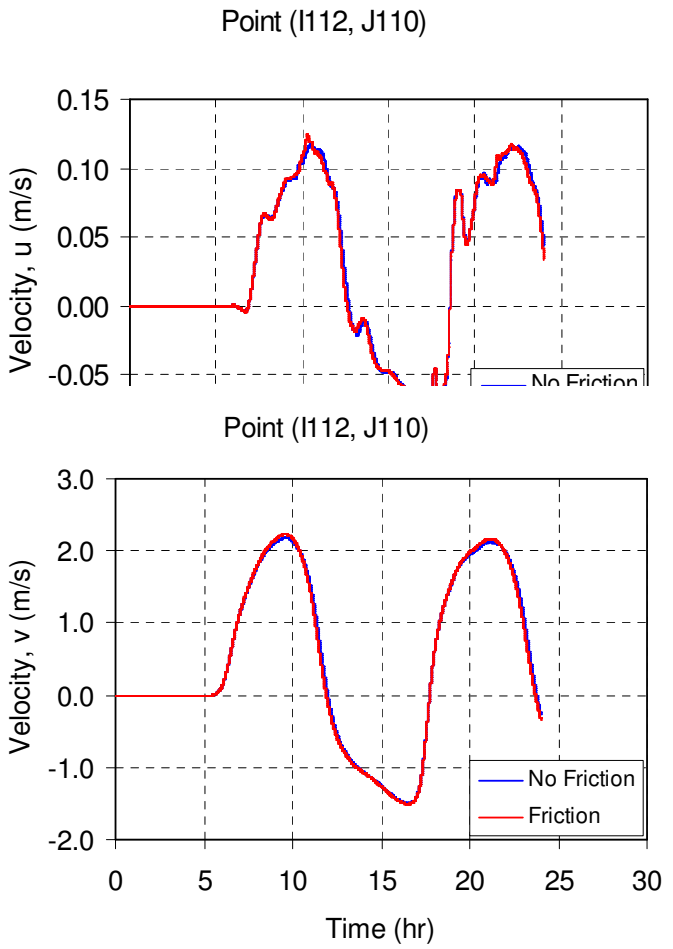

In order to look into the cause, the flooding situations for both calculations including and excluding mangrove drag resistance are investigated. The calculation shows that the flooding water (at 18hr 40min) enters deeper inside the swamp near the estuary mouth if the flood plain is assumed to be no resistance except the bed friction (Figure 5). This large expansion of the flooding will cause a reduction of water mass entering into the midstream creek region. This volume reduction effect will exceed the resistance effects by mangrove roots, and this is the reason that the results of including roughness yield the greater velocities.

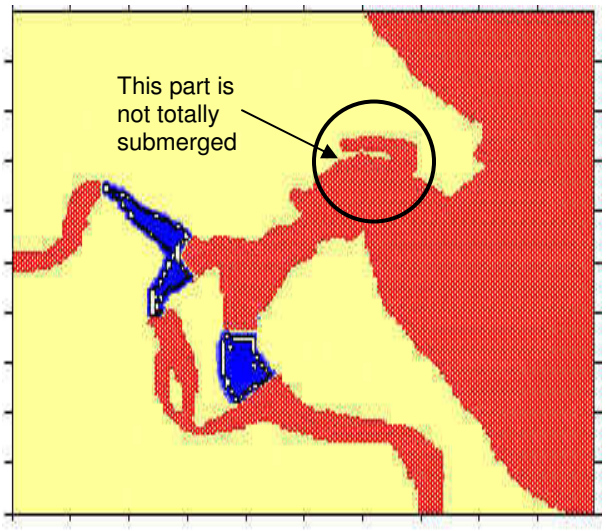

Figure 5a. Flooding conditions including mangrove drag resistance

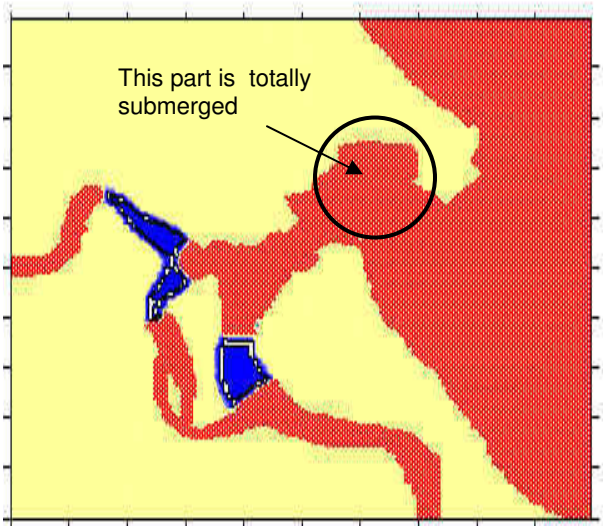

Figure 5b. Flooding conditions excluding mangrove drag resistance

CONCLUSIONS

The estimated drag resistance in terms of Manning rough coefficient is found to be consistent with that suggested by the existing knowledge of open channel flow for vegetated flood plains. The peak values of velocity fluctuations are reduced by an occurrence of flooding, and the temporal fluctuations are slightly skewed to lean backward. The unexpected result is observed on the study of drag resistance

effects on the water level and velocity fluctuations. The retarding effects on the creek velocity does not appear, even on the contrary, the peak velocity including the mangrove drag resistance becomes slightly greater than that no drag resistance assumed. The reason is that more flooding water intrusion occurs in the swamp near the estuary mouth when the mangrove drag resistance is ignored.

ACKNOWLEDGEMENTS

This research was conducted with joint funding from the Malaysian Ministry of Science under the Intensified Research for Priority Areas (IRPA) and Japanese Ministry of Education, Science, Sports and Culture (MONBUSHO). The authors wish to express their gratitude to Kartini Mohamed, Haji Sukiman, and Dr. Kamaruzzaman Hj. Yunus for their invaluable assistance and hospitality throughout the sampling period.

REFERENCES

Asano, T., Saad, S., and Husain, L.M. (2000). Hydrodynamics in tidal creeks – mangrove swamp system in Kemaman Estuary, Malaysia. Hydrodynamics IV. *Proc. Of the Fourth Int. Conf. On Hydrodynamics, Yokohama.* Pp. 771-776

Furukawa, K. and Wolanski, E. (1996). Sedimentation in mangrove forest. J. Mangrove and Salt Marshes. 1 (1): pp. 3-10

Saad, S., Husain, L.M., Yaacob, R., and Asano, T. (1999). Sediment accretion and variability of sedimentological characteristics of a tropical estuarine mangrove: Kemaman, Terengganu, Malaysia. *Mangroves and Salt Marshes*. 3: pp. 51-58.

Stumpf, R. P. (1983). The processes of sedimentation on the surface of salt marsh. Estuar., Coast and Shelf Sci. 17: pp. 495 - 508